Available online at www.sciencedirect.com

ScienceDirect

Procedia Structural Integrity 42 (2022) 1336–1343

Structural Integrity Procedia

www.elsevier.com/locate/procedia

23 European Conference on Fracture - ECF23

Impact of conductor assembly indentation on the fatigue properties of copper power cable wires

Luigi Mario Viespoli[1] *, Audun Johanson[2], Stéphane Dumoulin[1], Anette Brocks Hagen[1], Di Wan[3], Filippo Berto[3], Antonio Alvaro[1,3]

[1]*Department of Materials and Nanotechnology, SINTEF Industry, 7456, Trondheim, Norway*
[2]*Nexans Norway, Freserveien 1, 0196 Oslo Norway*
[3]*Department of Mechanical and Industrial Engineering, Norwegian University of Science and Technology (NTNU), 7491 Trondheim, Norway*

Abstract

The production process of high voltage power cables includes the assembly of the conductor, which is composed of different layer of independent wires wound in helixes of opposite pitch for each subsequent layer. Each wire, which has an initial constant round cross section and is close to annealed conditions, is wound around the previous layer and the assembled layers are passed through a calibrated die which compacts the wires together. This process creates periodically spaced indents on the inner side of the wires and work hardens the material in the indented sections and their immediate proximity. Both the local and global strain distribution related to static loads as well as the fatigue properties of the wires are impacted by such process and its consequent geometrical and material inhomogeneities. In this work, strain-control fatigue results of copper conductor wire are presented. The non-uniform strain distribution caused by the inhomogeneities inferred by their manufacturing process is investigated with the means of digital image correlation. The "indentation" process is modelled with the use of explicit finite elements and the deformation of the virtual specimen obtained is compared with the experimental results.

Keywords: Copper, residual stresses, fatigue, modelling.

* Corresponding author. *E-mail address:* luigi.viespoli@sintef.no

10.1016/j.prostr.2022.12.170

1. Introduction

In to the current and future foreseeable energy market, the relevance of electrification and interconnection of national grids is on the rise. This infers that subsea power cables, components of already strategically essential infrastructures, are becoming even more important. In particular, the production of renewable energy from sources such as floating wind turbines and wave energy harvesting, increases the need for reliable dynamic power cables. A cable used in a dynamic application must be able to reliably withstand fatigue loading throughout its lifecycle. Conductor cores are often manufactured in Electrolytic Tough Pitch (ETP) copper, which is characterised by high purity and conductivity. Commercially pure copper has been the object of numerous studies, focused on its plasticity mechanisms and performance under fatigue loading: Jenkins and Digges (1951), Perlega (2015), Wan et al. (2022). In particular, Mughrabi (2010) offered an interesting summary of strain-controlled copper fatigue results, while Karlsen (2010) provided a study specifically on fatigue of copper conductors. A stranded conductor consists of a bundle of wires which are assembled layer after layer in a helical pattern. After the addition of each layer, the bundle is passed through a calibrated vice, which compacts the wires increasing the volume share occupied by conductive material. Such operations cause localised deformation and hardening at the contact points, leaving a series of periodic indentation marks on the wires. These indents and their impact on the fatigue performances of the wires are the focus of the present work. Fatigue results of individual wire are presented, and the uneven strain distribution measured along the length of the wires is discussed. Explicit FE modelling of the indentation process, as well as of the pre-straining and of the initial cyclic loading were performed to better understand the stress-strain status caused by the production process and its impact on deformation of the specimens during fatigue testing. As a relatively straightforward approach, the Signed von Mises equivalent stress range has been evaluated by some authors as relevant parameter through which to perform fatigue analysis of components under complex loading: Engin and Coker (2017), Gates and Fatemi (2015), Papuga et al. (2012). This method has been applied to the wire indents in this work. The impact of creep relaxation was neglected during the numerical modelling, as well as fretting between different layers of conductor, which will be the scope of a separate work.

2. Fatigue testing results and numerical study background

Fatigue testing in displacement control on wire samples, monitored with DIC, has demonstrated the uneven distribution of the applied deformation. Both the initial pre-strain and the fatigue strain amplitude are not constant through the length of the specimen but concentrated in specific areas (Figure 1 a), which depend and relate to the indentation of the wire (Figure 1 b). The indentation process causes work hardening in the section of cable where the inner wire layer is pressed, while the sections in between remain in the softer initial condition. We define therefore three strains measurements obtained through Digital Image Correlation (DIC) technique, according to the regions shown in Figure 1 a: a Minimum, a Maximum and a Global (or Nominal) strain, which is the average over a period of wire. During the pre-straining phase, the Global applied strain is distributed unevenly across these regions, as shown in Figure 1 c. Observing the evolution of the DIC results for the mean strain over time, it is recorded that if the mean Global strain is kept constant, the softer region (Max) will keep absorbing deformation due to creep, while the hardened part (Min) will release part of its elastic deformation (Figure 1 c). Also, the strain amplitude is unevenly distributed on these regions, but to a far lower extent than the level recorded during the pre-strain phase (Figure 1 d). Since the material is subjected to creep deformation and tested in displacement control, the mean stress will relax towards zero, provided that the test is sufficiently long (Figure 1 e). On the other hand, the stress range is not observed to vary significantly during tests.

The fatigue testing was performed in displacement control in a Zwick LTM 10 electro-dynamic testing machine, in air at a temperature of 90 °C, that is a typical operating temperature for conductor cores. Tests were performed on different layer wires at a frequency of 20 Hz to identify the impact of assembly position on the fatigue life of the ETP copper tested. The summary of the fatigue testing results is given by Figure 2 (a), together with an example of fracture surface showing part of an indent (b). The results are presented in terms of DIC mean strain range versus cycles to failure for the different layers and frequencies tested. The central, outer and outer minus one layers are indicated as C, O and O-1 respectively. Full markers indicate tests failed in the gauge length, while empty markers indicate runouts or interrupted tests (i.e., grip failure). The specimens consisted in individual wire sections of a length sufficient to

contain 3 indentation periods, i.e. 30 mm, while the average cross section of each wire was 9.88 mm^2. The samples were gripped by collets without the possibility to reduce the cross section in the gauge length in order to avoid any significant modification of the overall wire geometry. However, this posed considerable challenges due to the weakness of the gripping region. The following testing procedure was applied: warming up the sample until equilibrium (>30'), pre-straining phase (targeting 0.5 % deformation), cyclic loading in displacement control until failure. The central wire revealed a minimal work hardening in production and, above all, presented no inhomogeneity, neither geometrically, nor in the hardening distribution. Intuitively, this could lead to suspect a far better performance of this layer compared to the outer ones. On the contrary, the fatigue testing results show a minimal reduction of fatigue life for the indented wires when compared to the central ones. From a practical viewpoint, this signifies that the exact conductor design and degree of compaction for each individual wire at least to the extent here tested, should have a limited impact in fatigue life estimates.

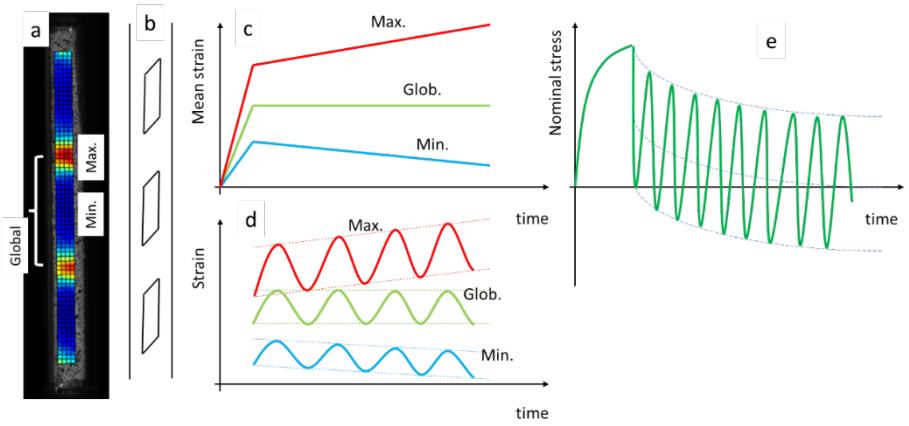

Fig. 1. Schematic definition of Global, Maximum and Minimum strain on DIC strain map (a) with respect to indent location (b) and typical time evolution (c, d). Typical time evolution of Nominal Stress (e).

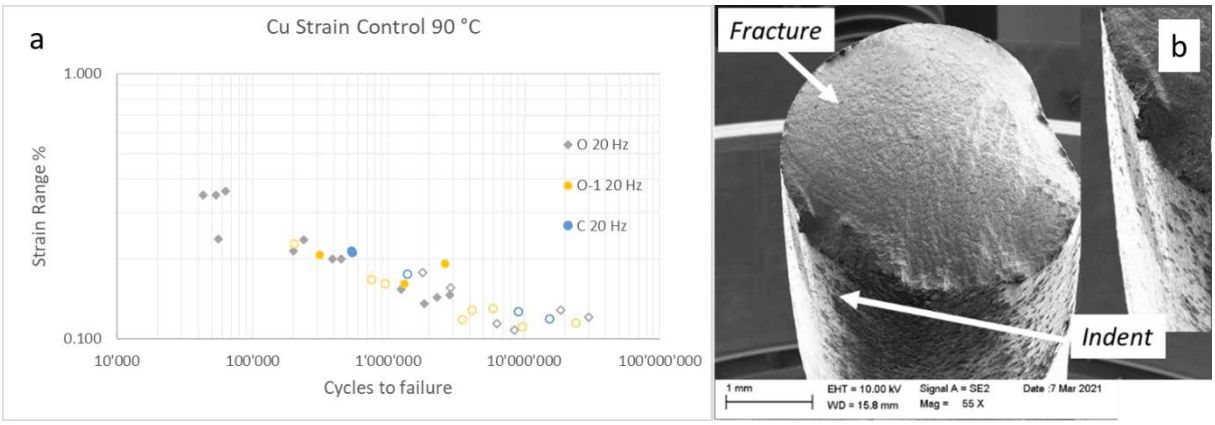

Fig. 2. (a) Fatigue results for different wire layers. (b) SEM image of indent and typical fatigue fracture.

3. Indentation modelling

3.1. Indentation process and residual stress

In order to gain a deeper understanding of the strain distribution when the material is subjected to the deformation imposed during the aforementioned test procedure, an approximation of the indentation process of the outermost layer of the conductor and of the pre-strain and initial fatigue cycles was modelled for some representative conditions. The starting point for the material properties is the tensile curve of the alloy of interest under annealed conditions, obtained from the testing of a wire in the central position of the cable (Figure 3). For the purpose of this analysis, performed in ABAQUS with a dynamic explicit solver for stability, time dependent plasticity was neglected. The analysis was articulated in three steps: indentation, removal of the indentation parts and pre-straining plus initial cycles. The first two steps recreate the specimen in testing conditions and are the object of this paragraph. When the cable conductor is assembled, each subsequent layer of wires is wrapped on the precedent (in the order 1, 6, 12, 18 and so on) and passed through a calibrated vice which increases the conductor volume fraction plastically deforming the wires and slightly reducing the diameter. The wire is pressed among the inner, already hardened, layer, the neighbouring wires and the tool on the outside, reproducing the process of the formation of the periodic indents. Figure 3 (b) shows how the different elements involved in the process have been approximated: a section of wire of length corresponding one period of indentation (1), a vice representing the tool and the neighbouring wires (2), the hardened wire of the inferior layer (3). The relative angle between the longitudinal directions of parts 1 and 3 in Figure 3 was set to the angle between the longitudinal axis of the two wires in the contact points, while the displacement imposed for the deformation was adjusted in order to obtain the same minimum thickness in the FEM indented section as in the real wire. Parts 2 and 3 are then removed from the simulation to proceed with the last step, the modelling of pre-straining and of the initial cycles. Figures 4 shows a cut-out of the wire in after indentation, representing hydrostatic pressure (a) and plastic equivalent strain (b). It is evident how, in order to reach a given target deformation level, a considerable portion of material under the contact area has reached stresses greater than yield and therefore underwent considerable permanent deformation.

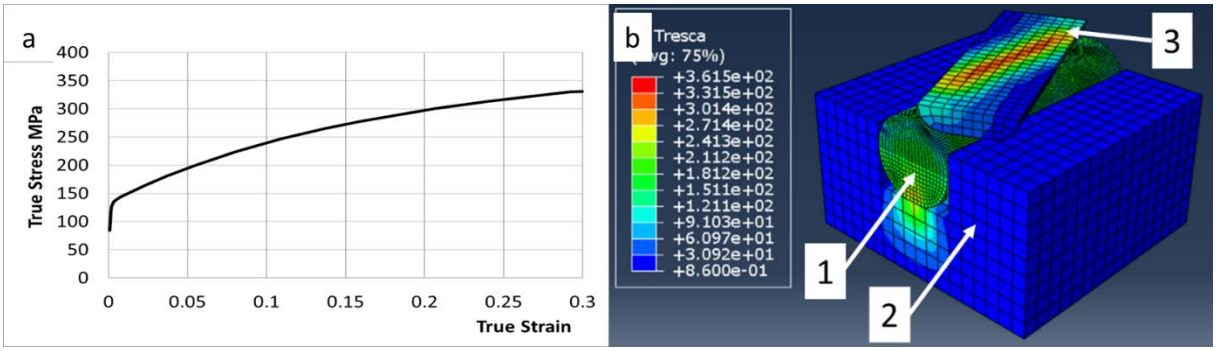

Fig. 3. (a) Reference tensile curve used for the simulations. (b) Parts involved in the indentation process: wire (1), tool and neighbouring wires (2), wire inner layer (3).

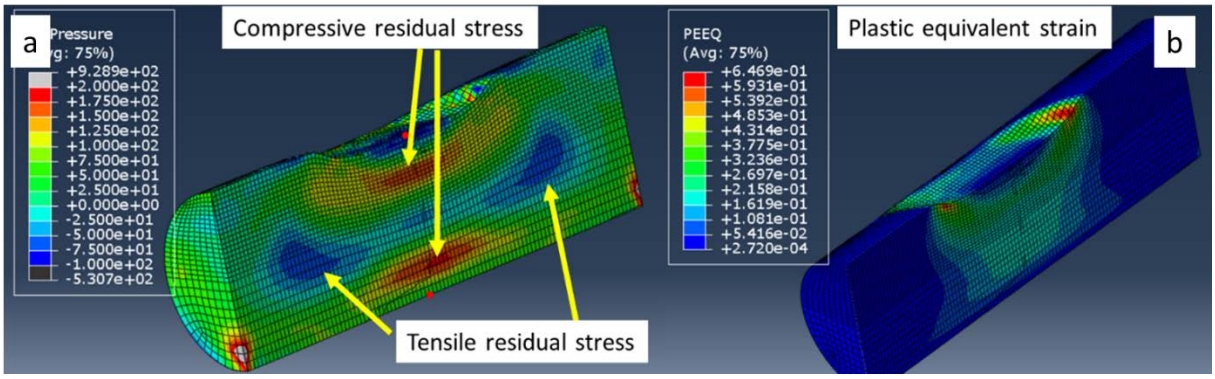

Fig. 4. Stress-strain status of the wire after indentation: pressure (a), plastic equivalent strain (b).

3.2. Pre-straining and cycling loading

The last step of the simulation is tailored to model the initial part of the loading procedure in the experiments: the pre-straining and the initial fatigue cycles. The indent formed in the first step is clearly visible in Figure 5 (a), while the areas on which the three strains are extracted are shown in Figure 5 (b), and are defined on the opposite, flat surface, analogously to what was done for the actual specimen (Figure 1). Any combination of pre-strain and strain range can be applied so to directly compare the modelling results to those revealed by the DIC postprocessing of the actual tests. The displacement is applied varying linearly in the step time, time which does not scale 1:1 with the real test time, but which has been adjusted to the smallest possible value, containing kinetic effects to an acceptable level, for computational efficiency. Figure 6 (a) shows the evolution, for an example testing condition, of the three strain values in the dynamic explicit step, while Figure 6 (b) shows the nominal stress to be applied (referring to the initial cross section) in order to obtain the required displacement. For low nominal stress values, the difference between the three strain types is minimal while, at the step time at which the stress deviates from linearity, the strain curves diverge. This stress value is slightly higher than the yield stress of the tensile curve assumed as base material property (Figure 3a), indicating that some section of the material has undergone hardening in the process. This area corresponds to the one from which the Minimum strain is extracted, and its hardening is clearly visible from the cut-out plastic equivalent strain plot in Figure 4. In Figure 6 (a), we can observe a great difference in the amount of pre-strain absorbed by the different regions of the wire, while the difference on the strain range is less pronounced, as seen from the DIC analysis of test data.

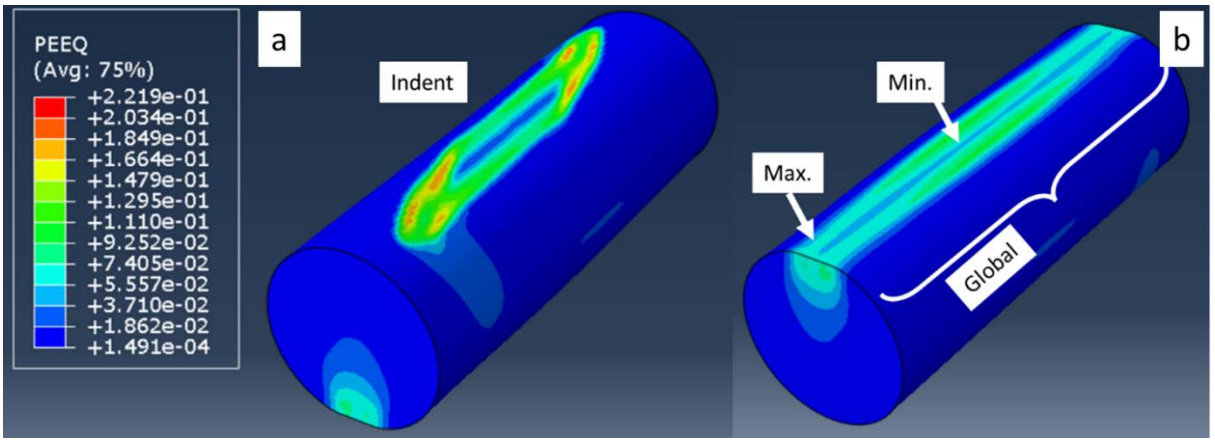

Fig. 5. Indent location (a) with respect to the areas of extraction of "Global", "Maximum" and "Minimum" strain (b).

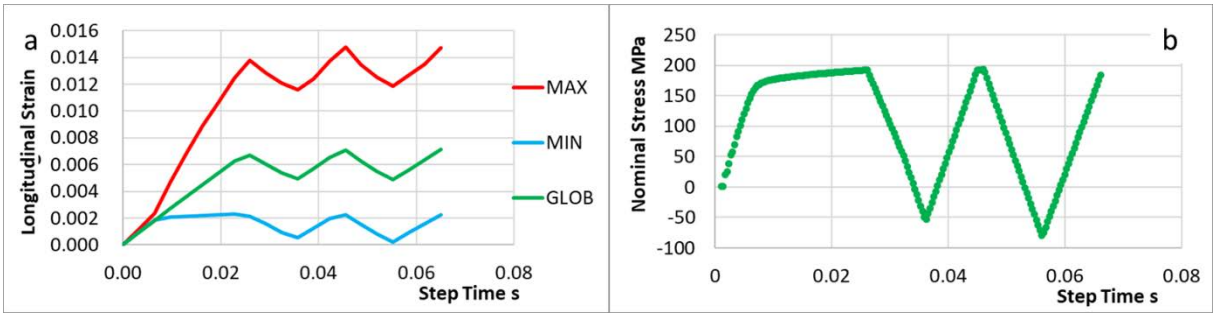

Fig. 6. Example of FEM strain distribution (a) and nominal stress evolution (b) for global pre-strain 0.5 % and global strain range 0.22 %. Note: the step time does not scale 1:1 with real testing time.

3.3. Validation by comparison with experimental results

It is necessary to validate the models comparing their ability to reproduce the work hardening localization induced by the process with the available experimental results. The parameter selected for this evaluation is the relative difference, in percent, between the Minimum and Maximum strains, both for the pre-strain and for the strain range, as a function of the applied Global value of pre-strain or strain range respectively. Figure 7 shows these data plotted for two sets: the FEM results (bigger bullet points) and the experimental results (smaller bullet points). The experimental data have a relatively high scatter, which is attributed to a series of factors: local microstructural and geometrical differences between the samples and to noise in the DIC analysis. However, a clear trend is shown: the accumulation of pre-strain in the non-hardened area has a high value and is, as intuitively expected, proportional to the amount of pre-strain applied, while the strain range is more equally distributed and not clearly affected by the pre-strain. The FEM results have been generated for three representative combinations of global pre-strain and strain amplitude. The results of the simulations fall within the cloud of experimental results, indicating the models are valid for being used as support in the understanding of the stress/strain conditions in the indented wire.

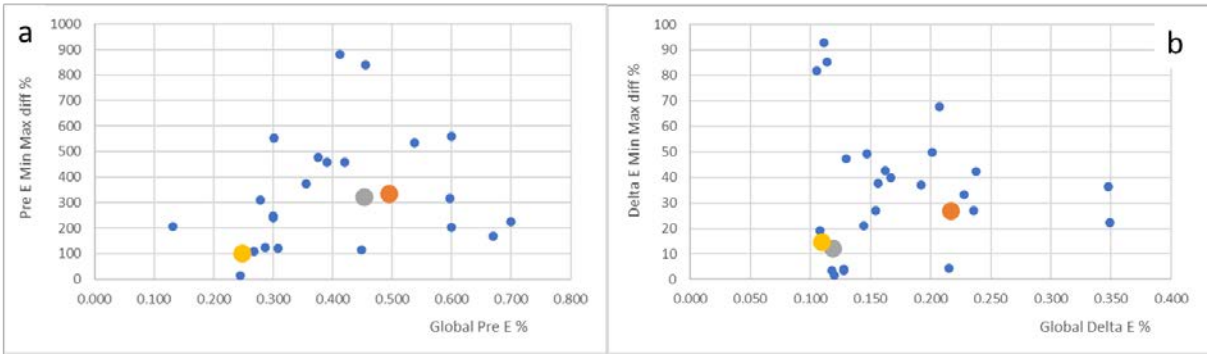

Fig. 7. (a) Ratio between Min and Max pre-strain as a function of the Global pre-strain. (b) Ratio between Min and Max strain range as a function of the Global strain range. The small blue dots correspond to the experimental values, while the other bigger three dots correspond to 3 different modelled combinations of pre-strain and strain range.

3.4. Signed von Mises stress range analysis

The indentation process causes, as seen in the previous paragraphs, not only a geometrical stress concentrator, but also a complex distribution of work hardening and residual stresses. In addition the plastic deformation inherent to the pre-straining should be accounted for. It is evident how the precise local loading condition in the indent and in its proximity is difficult to establish and it would require a more sophisticated approach for the interpretation of fatigue

results. In this work, the signed von Mises stress range method was applied, but it delivered overconservative results. The well-known von Mises equivalent stress is a yielding criterion based on the distortion energy. Its value is, by definition, always positive and therefore it does not distinguish whether a stress state is caused by a predominantly tensile or compressive loading. The signed von Mises equivalent stress range tries to overcome this limitation by attributing a sign to the von Mises stress and then computing its range over the loading cycle. Different parameters have been tried (hydrostatic pressure p, maximum principal stress S1 and principal stress of greater magnitude) with the maximum principal stress providing the most reasonable results. The formulation applied was therefore:

$$\sigma_{Mises} = \frac{1}{\sqrt{2}}\sqrt{(\sigma_1 - \sigma_2)^2 + (\sigma_1 - \sigma_3)^2 + (\sigma_2 - \sigma_3)^2} \quad (1)$$

$$Signed\ \sigma_{Mises} = sign(S_1) \cdot \sigma_{Mises} \quad (2)$$

$$\Delta Signed\ \sigma_{Mises} = max(Signed\ \sigma_{Mises}) - min(Signed\ \sigma_{Mises}) \quad (3)$$

The stress state was extracted from the FE output file for each time increment and each element in the specimen. The given definition of equivalent stress range was then applied. The equivalent stress range obtained vs element count is shown in Figure 8 for two different loading conditions, together with the nominal stress range. In the case of the smaller applied strain ranges, the nominal stress range is exceeded slightly by a few elements, while in the case of the greater strain ranges, the equivalent stress range computed is significantly higher than the nominal one for a great portion of elements. The degree of stress amplification provided by the applied method is such that, had the results been realistic, a shorter fatigue life than those obtained through testing would have been expected for ETP copper in absence of the indents. On the contrary, the testing depicted a much brighter picture on the impact of the indents than this numerical postprocessing. In both postprocessing a few "flyers" can be seen, that is elements whose equivalent stress range is strangely above the rest of the data. These are the results of particular combinations in which the first principal stress barely changes sign but causes a great difference between the maximum and minimum signed equivalent stress.

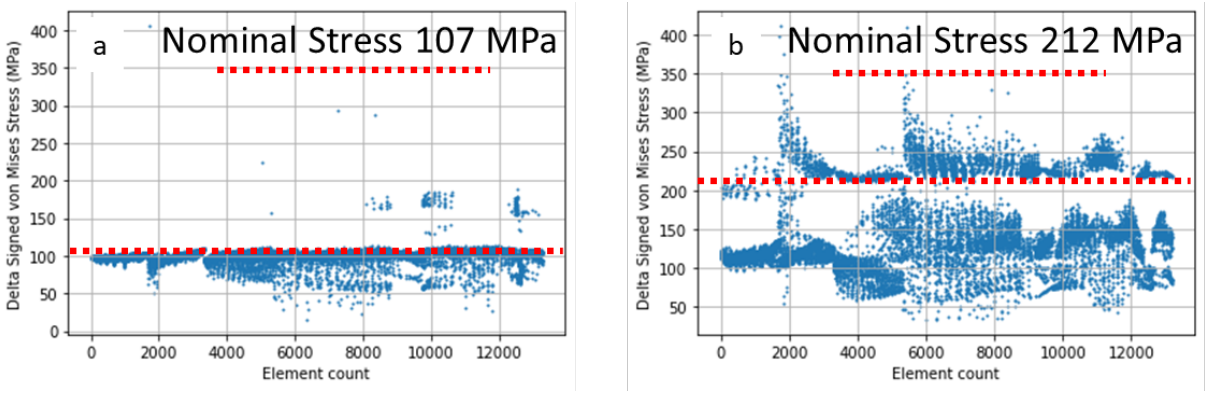

Fig. 8. Equivalent stress range vs nominal stress range for each element for two loading conditions: pre-strain of 0.5 % and strain range of 0.11 % (a) and pre-strain of 0.55 % and strain range of 0.22 % (b).

4. Conclusions

In this work, some aspects related to the fatigue behaviour of subsea power cables are analysed. ETP copper wires extracted from actual conductor cores were subjected to displacement-controlled fatigue at the typical operating temperature of 90 °C and a frequency of 20 Hz. It was observed that the indents cause an uneven strain distribution in the samples and that the fracture propagation plane often cuts through them. Moreover, creep relaxation is relevant for this type of copper and continues until the mean stress becomes negligible. The fatigue results obtained on the

central wire, which is not affected by geometrical and hardening inhomogeneity, present a minimal performance improvement compared to the indented outer layers. Consequentially, the exact conductor design and degree of compaction shall have a limited impact on the fatigue life estimation. A numerical study was performed to gain a better understanding of the hardening level and residual stress condition of the wire after the indentation process, and how this affects the pre-strain and strain range distribution during fatigue loading. The models created could approximate the behaviour observed in the testing in a satisfactory manner. In addition, the signed von Mises stress range was used as a relatively straightforward method to postprocess the cyclic loading results and quantify the impact of the indents but provided overconservative results. The effect of creep relaxation at the indents has been neglected in this work but will be considered in the future. Time dependent plasticity modelling and residual stress measurement are strongly recommended to be implemented. Last but not least, fretting fatigue between different layers of the cable is a complex and important topic which was excluded from this work but will be investigated in the future.

Acknowledgements

This work is financed by the Research Council of Norway and the industrial partners Nexans Norway through the NASCAR industrial research project.

References

W.D. Jenkins, T.G. Digges, Creep of annealed and cold-drawn high-purity copper, J. Res. Natl. Bur. Stand. 47 (4) (1951) 272–287.

A. Perlega, Influence of Testing Frequency on the Fatigue Properties of Polycrystalline Copper, Institut für Festk¨orperphysik, TU Wien, 2015.

Di Wan, Anette Brocks Hagen, Luigi Mario Viespoli, Audun Johanson, Filippo Berto, Antonio Alvaro, In-situ tensile and fatigue behavior of electrical grade Cu alloy for subsea cables, Materials Science and Engineering: A, Volume 835, 2022.

Hael Mughrabi, Fatigue, an everlasting materials problem - still en vogue, Procedia Engineering, Volume 2, Issue 1, 2010.

Karlsen, S. "Fatigue of Copper Conductors for Dynamic Subsea Power Cables." Proceedings of the ASME 2010 29th International Conference on Ocean, Offshore and Arctic Engineering. 29th International Conference on Ocean, Offshore and Arctic Engineering: Volume 6. Shanghai, China. June 6–11, 2010

Zafer Engin, Demirkan Coker, Comparison of Equivalent Stress Methods with Critical Plane Approaches for Multiaxial High Cycle Fatigue Assessment, Procedia Structural Integrity, Volume 5, 2017.

Gates, Nicholas & Fatemi, Ali. (2015). Fatigue Life of 2024-T3 Aluminum under Variable Amplitude Multiaxial Loadings: Experimental Results and Predictions. Procedia Engineering.

Papuga J., Vargas M., Hronek M.: Evaluation of Uniaxial Fatigue Criteria Applied to Multiaxially Loaded Unnotched Samples. Engineering MECHANICS, Vol. 19, 2012, No. 2/3.